

The International Journal Of Microcircuits And Electronic

Volume No. 12

Issue No. 2

May - August 2024



ENRICHED PUBLICATIONS PVT.LTD

**JE - 18,Gupta Colony, Khirki Extn,
Malviya Nagar, New Delhi - 110017.**

E- Mail: info@enrichedpublication.com

Phone :- +91-8877340707

The International Journal Of Microcircuits And Electronic

Aims and Scope

The International Journal of Microcircuits And Electronic is a journal that publishes original research papers in the fields of microcircuits, microelectronics, multichip module technologies, electronic materials, surface mount and other related technologies, interconnections, RF and microwaves, wireless communications, manufacturing, design, test, and reliability
and more...

Formerly : EP Journal of Microcircuits and Electronic

The International Journal Of Microcircuits And Electronic

**Managing Editor
Mr. Amit Prasad**

Editorial Board Member

S. Gajendran

Associate Professor/Production Engineering
MIT, Anna University, Chennai,
India
gajendrasm@gmail.com

The International Journal Of Microcircuits And Electronic

(Volume No. 12, Issue No. 2, May - August 2024)

Contents

Sr. No.	Articles/ Authors Name	Pg. No.
1	Biometric Security Using Iris Recognition: A Survey <i>- Rushikesh M. Shete, Sunny Gandhi, Sagar Badiye</i>	1 - 8
2	Cost Effective Retrofitting Of 12 Pulse AC-DC Converter Using 24 Pulse AC-DC Converter <i>- R.Suguna, S.Navadeep, D.Banupriya</i>	9 - 18
3	Series Combination Of Hybrid Filter With Distorted Source Voltage <i>- S. Dineshkumar</i>	19 - 26
4	Power Efficiency Improvement Method For A BI- Directional Dual Active Bridge DC-DC Converter <i>- K. Divya</i>	27 - 34
5	Design Of Embedded System Based Rapid Sensing AC Electrical Capacitance Tomography <i>- K. Manikandan, S. Sathiyamoorthy</i>	35 - 41

Biometric Security Using Iris Recognition: A Survey

Rushikesh M. Shete*, **Sunny Gandhi****, **Sagar Badiye*****

* Computer Sci. & Engineering, Dept., D.M.I.E.T.R Sawangi(M), Wardha

** Information Technology Dept. DMIETR, Sawangi (M), Wardha

*** Department of CSE, YCCE, Nagpur, RTMNU, Nagpur, India

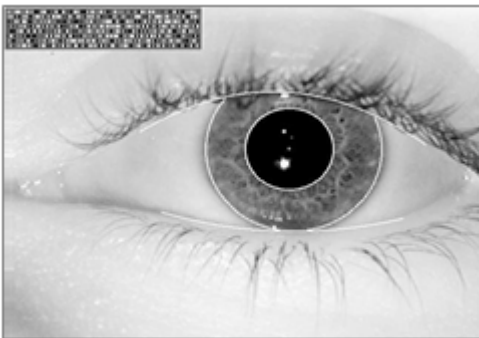
ABSTRACT

The Algorithm for Iris recognition was developed by Dr. John Daugman, University Of Cambridge. The iris tests have been tested on over 6 million people with no false results. The recognition principle is the failure of a test of statistical independence on iris phase structure encoded by multi-scale quadrature wavelets. This paper explains the iris recognition algorithm that is being used today in various fields.

I. INTRODUCTION

Reliable automatic recognition of persons has long been an attractive goal. As in all pattern recognition problems, the key issue is the relation between inter class and intra-class variability: objects can be reliably classified only if the variability among different instances of a given class is less than the variability between different classes. Iris recognition technology combines computer vision, pattern recognition, statistical inference, and optics. Its purpose is real-time, high confidence recognition of a person's identity by mathematical analysis of the random patterns that are visible within the iris of an eye from some distance. Because the iris is a protected internal organ whose random texture is stable throughout life, it can serve as a kind of living passport or a living password that one need not remember but can always present. Because the randomness of iris patterns has very high dimensionality, recognition decisions are made with confidence levels high enough to support rapid and reliable exhaustive searches through national-sized databases. The algorithms for iris recognition were developed at Cambridge University by John Daugman. Example of an iris pattern, image. monochromatically at distance of about 35 cm. The outline overlay shows results of the iris and pupil localization & eyelid detection steps. Iris patterns become interesting as an alternative approach to reliable visual recognition of persons when imaging can be done at distances of less than a meter, and especially when there is a need to search very large databases without incurring any false matches

despite a huge number of possibilities. Although small (11 mm) and sometimes problematic to image, the iris has the great mathematical advantage that its pattern variability among different persons is enormous. In addition, as an internal (yet externally visible) organ of the eye, the iris is well protected from the environment and stable over time. As a planar object its image is relatively insensitive to angle of illumination, and changes in viewing angle cause only affine transformations; even the non affine pattern distortion caused by pupillary dilation is readily reversible. Finally, the ease of localizing eyes in faces, and the distinctive annular shape of the iris, facilitate reliable and precise isolation of this feature and the creation of a size- invariant representation.



The major applications of this technology so far have been:

- substituting for passports,
- aviation security
- controlling access to restricted areas at airports
- computer login
- Access to buildings and homes.

The largest single current deployment of these algorithms is in the United Arab Emirates, where every day about 2 Billion iris comparisons are performed. All travellers arriving at all 17 air, land, and sea ports have their Iris Codes quickly computed and compared against all the Iris Codes in a large database, within about 2 seconds.

II. LOCATING THE IRIS

To capture the rich details of iris patterns, an imaging system should resolve a minimum of 70 pixels in iris radius. In the held trials to date, a resolved iris radius of 100 to 140 pixels has been more typical. Monochrome CCD cameras (480 x 640) have been used because NIR illumination in the 700nm 900nm band was required for imaging to be invisible to humans. Some imaging platforms deployed a wide angle camera for coarse localization of eyes in faces, to steer the optics of a narrow-angle pan/tilt camera that acquired higher resolution images of eyes. There exist many alternative methods for finding and tracking facial features such as the eyes, and this well researched topic will not be discussed further here. In the setrials, most imaging was done without active pan/tilt camera optics, but instead exploited visual feedback via a mirror or video image to enable cooperating Subjects to position their own eyes within the field of view of a single narrow-angle camera. Focus assessment was performed in real-time(faster than video frame rate) by measuring the total high-frequency power in the 2D Fourier spectrum of each frame, and seeking to maximize this quantity either by moving an active lens or by providing audio

feedback to Subjects to adjust their range appropriately. Images passing a minimum focus criterion were then analyzed to find the iris, with precise localization of its boundaries using a coarse-to-fine strategy terminating in single-pixel precision estimates of the center coordinates and radius of both the iris and the pupil. Although the results of the iris search greatly constrain the pupil search, concentricity of these boundaries cannot be assumed. Very often the pupil center is nasal, and inferior, to the iris center. Its radius can range from 0.1 to 0.8 of the iris radius. Thus, all three parameters defining the pupillary circle must be estimated separately from those of the iris. A very effective integro differential operator for determining these parameters is:

$$\max_{(r, x_0, y_0)} \left| G_{\sigma}(r) * \frac{\partial}{\partial r} \oint_{r, x_0, y_0} \frac{I(x, y)}{2\pi r} ds \right|$$

Where, $I(x; y)$ is an image such as Fig 1 containing an eye. The operator searches over the image domain $(x; y)$ for the maximum in the blurred partial derivative with respect to increasing radius r , of the normalized contour integral of $I(x; y)$ along a circular arc ds of radius r and center coordinates $(x_0; y_0)$. The symbol $*$ denotes convolution and $G_{\sigma}(r)$ is a smoothing function such as a Gaussian of scale σ . The complete operator behaves in effect as a circular edge detector, blurred σ , at a scale set by which searches iteratively for a maximum contour integral derivative with increasing radius at successively finer scales of analysis through the three parameter space of center coordinates and radius $(x_0; y_0; r)$ defining a path of contour integration. The operator in (1) serves to find both the pupillary boundary and the outer (limbus) boundary of the iris, although the initial search for the limbus also incorporates evidence of an interior pupil to improve its robustness since the limbic boundary itself usually has extremely soft contrast when long wavelength NIR illumination is used. Once the coarse-to-fine iterative searches for both these boundaries have reached single pixel precision, then a similar approach to detecting curvilinear edges is used to localize both the upper and lower eyelid boundaries. The path of contour integration in (1) is changed from circular to accurate, with spline parameters fitted by standard statistical estimation methods to describe optimally the available evidence for each eyelid boundary. The result of all these localization operations is the isolation of iris tissue from other image regions, as illustrated in Fig by the graphical overlay on the eye.

III. LOCATION OF IRIS REGARDLESS OF SIZE, POSITION AND ORIENTATION

Robust representations for pattern recognition must be invariant to changes in the size, position, and orientation of the patterns. In the case of iris recognition, this means we must create a representation that is invariant to the optical size of the iris in the image (which depends upon the distance to the eye, and the camera optical magnification factor); the size of the pupil within the iris (which introduces a non-affine

pattern deformation); the location of the iris within the image; and the iris orientation, which depends upon head tilt, torsional eye rotation within its socket (cyclovergence), and camera angles, compounded with imaging through pan/tilt eye-finding mirrors that introduce additional image rotation factors as a function of eye position, camera position, and mirror angles. Fortunately, invariance to all of these factors can readily be achieved.

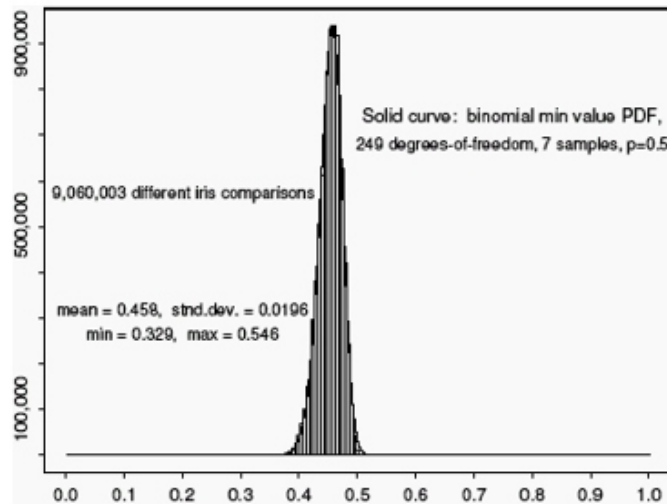


Figure 3.1 Distribution of Hamming distances

For on-axis but possibly rotated iris images, it is natural to use a projected pseudo polar coordinate system. The polar coordinate grid is not necessarily concentric, since in most eyes the pupil is not central in the iris; it is not unusual for its nasal displacement to be as much as 15%. This coordinate system can be described as doubly-dimensionless: the polar variable, angle, is inherently dimensionless, but in this case the radial variable is also dimensionless, because it ranges from the pupillary boundary to the limbus always as a unit interval $[0, 1]$. The dilation and constriction of the elastic meshwork of the iris then the pupil changes size is intrinsically modeled by this coordinate system as the stretching of a homogeneous rubber sheet, having the topology of an annulus anchored along its outer perimeter, with tension controlled by an (off-centered) interior ring of variable radius. The homogeneous rubber sheet model assigns to each point on the iris, regardless of its size and pupillary dilation, a pair of real coordinates $(r; \theta)$ where r is on the unit interval $[0, 1]$ and θ is angle $[0, 2\pi]$. The remapping of the iris image $I(x, y)$ from raw Cartesian coordinates $(x; y)$ to the dimensionless non concentric polar coordinate system $(r; \theta)$ can be represented as

$$I(x(r, \theta), y(r, \theta)) \rightarrow I(r, \theta)$$

Where, $x(r; \theta)$ and $y(r; \theta)$ are defined as linear combinations of both the set of pupillary boundary points $(x_p(\theta); y_p(\theta))$ and the set of limbus boundary points along the outer perimeter of the iris $(x_s(\theta); y_s(\theta))$

bordering the sclera, both of which are detected by finding the maximum of the operator (1).

$$x(r; \theta) = (1 - r)x_p(\theta) + rx_s(\theta)$$

$$y(r; \theta) = (1 - r)y_p(\theta) + ry_s(\theta)$$

Since the radial coordinate ranges from the iris inner boundary to its outer boundary as a unit interval, it inherently corrects for the elastic pattern deformation in the iris when the pupil changes in size. The localization of the iris and the coordinate system described above achieve invariance to the 2D position and size of the iris, and to the dilation of the pupil within the iris. However, it would not be invariant to the orientation of the iris within the image plane. The most efficient way to achieve iris recognition with orientation invariance is not to rotate the image itself using the Euler matrix, but rather to compute the iris phase code in a single canonical orientation and then to compare this very compact representation at many discrete orientations by cyclic scrolling of its angular variable. The statistical consequences of seeking the best match after numerous relative rotations of two iris codes are straightforward. Let $f_0(x)$ be the raw density distribution obtained for the HDs between different irises after comparing them only in a single relative orientation; for example, $f_0(x)$ might be the binomial defined in (4). Then $F_0(x)$, the cumulative of $f_0(x)$ from 0 to x , becomes the probability of getting a false match in such a test when using HD acceptance criterion x :

$$F_0(x) = \int_0^x f_0(x)dx$$

,

$$f_0(x) = \frac{d}{dx}F_0(x)$$

Clearly, then, the probability of not making a false match when using criterion x is $1 - F_0(x)$ after a single test, and it is $[1 - F_0(x)]^n$ after carrying out n such tests independently at n different relative orientations. It follows that the probability of a false match after a “best of n ” test of agreement, when using HD criterion x , regardless of the actual form of the raw unrotated distribution $f_0(x)$, is:

$$F_n(x) = 1 - [1 - F_0(x)]^n$$

and the expected density $f_n(x)$ associated with this cumulative is

$$\begin{aligned} f_n(x) &= \frac{d}{dx}F_n(x) \\ &= n f_0(x) [1 - F_0(x)]^{n-1} \end{aligned}$$

IV. ADVANTAGES AND DISADVANTAGES OF IRIS RECOGNITION

- Advantages of the Iris for Identification
- Highly protected, internal organ of the eye
- Externally visible; patterns imaged from a distance
- Iris patterns possess a high degree of randomness
 - o variability: 244 degrees-of-freedom
 - o uniqueness: set by combinatorial complexity
- Changing pupil size confirms natural physiology
- Limited genetic penetrance of iris patterns
- Patterns apparently stable throughout life
- Encoding and decision-making are tractable
 - o image analysis and encoding time: 1 second
 - o decidability index (d-prime): $d' = 7.3$ to 11.4
 - o search speed: 100,000 Iris Codes per second on 300MHz CPU

V. GENOTYPIC VERSUS PHENOTYPIC BIOMETRIC FEATURES

Genotype refers to a genetic constitution, or a group sharing it, and phenotype refers to the actual expression of a feature through the interaction of genotype, development, and environment. Genetic penetrance describes the heritability of factors, or the extent to which the features expressed are genetically determined. Those that are (such as blood group or DNA sequence) are called genotypic features, and those that are not (such as iris sequences, as shown above, or to a lesser degree fingerprints) I will call phenotypic features. The latter group may also be called epigenetic traits.

Persons who are genetically identical share all their genotypic features, such as gender, blood group, race, and DNA sequence. All biological characteristics of individuals can be placed somewhere along this "genotypic-phenotypic" continuum of genetic determination, with some features (e.g. gender; iris sequence) placed firmly at either endpoint. Other features such as facial appearance reveal both a genetic factor (hence identical twins "look identical") and an epigenetic factor (hence everyone's facial appearance changes over time).

Persons who share 50% of their genes (e.g. a parent and child; ordinary siblings; fraternal twins; and double cousins) show a corresponding partial agreement in their genotypic features such as facial appearance at a given age, but no additional agreement in their epigenetic features.

The importance of these genetic aspects of biometric templates is that they directly influence the two basic error rates: False Match and False non-Match. Nearly one percent of persons have an identical twin, with which they share all genotypic features such as their entire DNA sequence. This creates a minimum False Match rate of 1% (across a population) which we may call the biometrics' genotypic error rate. Similarly, the tendency for some biometric features (such as facial appearance) to change over time creates a minimum rate of False Rejections, which we may call the biometrics' phenotypic error rate. To maximize individuality, distinctiveness, and randomness, a biometric feature should be entirely epigenetic. To maximize stability over the life span, a biometric feature should not change with phenotypic development.

VI. COMPARISONS BETWEEN GENETICALLY IDENTICAL IRIS PATTERNS

Although the striking visual similarity of identical twins reveals the genetic penetrance of facial appearance, a comparison of genetically identical irises reveals just the opposite for iris patterns: the iris sequence is an epigenetic phenotypic feature, not a genotypic feature. A convenient source of genetically identical irises is the right and left pair from any given person. Such pairs have the same genetic relationship as the four irises of two identical twins, or indeed in the probable future, the $2N$ irises of N human clones. Eye color of course has high genetic penetrance, as does the overall statistical quality of the iris texture, but the textural details are uncorrelated and independent even in genetically identical pairs. This is shown in the Figure above, comparing 648 right/left iris pairs from 324 persons.

The mean Hamming Distance between genetically identical irises is 0.497 with standard deviation 0.031, which is statistically indistinguishable from comparisons between 9.1 million pairings of genetically unrelated irises. This shows that the detailed phase structure extracted from irises by the phasor demodulation process is purely epigenetic, so performance is not limited (as it is for face recognition, DNA, and some other biometrics) by the birth rate of identical twins or by the existence of partial genetic relationships.

Disadvantages of the Iris for Identification

- Small target (1 cm) to acquire from a distance (1 m)
- Moving target ...within another... on yet another
- Located behind a curved, wet, reflecting surface
- Obscured by eyelashes, lenses, reflections
- Partially occluded by eyelids, often drooping
- Deforms non-elastically as pupil changes size
- Illumination should not be visible or bright

VII. IRIDOLOGY

There is a popular belief in systematic changes in the iris patterns, reflecting the state of health of each of the organs in the body, one's mood or personality, and revealing one's future. Practitioners skilled in the art of interpreting these aspects of iris patterns for diagnosing clients' health, personality, and mutual compatibilities, are called iridologists. Like palm-readers, iridologists will offer advice on all of these matters (for a small fee) by inspecting your iris. Of course this is all just hocus-pocus; yet it is popular in California, around the Bay Area, and in parts of Europe such as Roumania

Some limited types of changes in iris appearance can occur and do have a scientific basis:

- (1) In the first few months of life, a blanket of chromatophore cells in the anterior layer of the iris establishes eye color; until this pigmentation develops, babies typically - even if only temporarily - have blue eyes.
- (2) Some pharmacological treatments for glaucoma involving prostaglandin analogues are reported to affect melanin, and therefore iris pigmentation, when applied topically to the eye. Such possible changes in iris color are irrelevant for the method of iris recognition described here, as imaging is done with monochrome cameras and using infrared illumination in the 700nm - 900nm band; melanin is almost completely non-absorbant at these wavelengths.
- (3) Freckles can develop over time in the iris, as elsewhere on the body. Again these are spots of melanin pigmentation, invisible in the infrared illumination used for iris recognition, so they neither help nor hinder in the identification of the iris pattern.
- (4) Elderly persons' eyes sometimes show a thin white ring surrounding the iris. This is an optical opacity that develops with age in the base of the cornea, where it joins the sclera.

VIII. BIBLIOGRAPHY

Complete Reference to Face Recognition Technique.
Iridology: A critical review. By L. Berggren.
Iris Recognition by Dr. Jaun Daugman, University Of Cambidge

Cost Effective Retrofitting Of 12 Pulse Ac-Dc Converter Using 24 Pulse AC-DC Converter

R. Suguna*, S. Navadeep*, D.Banupriya**

*Department of Electrical and Electronics, Muthayammal College of Engineering, Namakkal

**Department of Electrical and Electronics, Aadhithiya Institute of Technology, Coimbatore.

ABSTRACT

This paper proposes a new topology of multipulse converter which results in cost effective replacement of 12 pulse AC-DC converter by 24 pulse AC-DC converter, where 12 pulse converter is being used in industries. The proposed 24 pulse converter can reduce content of harmonics upto 21st level. The technique of pulse doubling is used to achieve 24 pulse from 12 pulse converter circuit. The pulse number is increased in order to decrease the harmonic content to meet the IEEE standard. According to IEEE, the permitted percentage of total harmonic distortion (THD) is below 5%. The topology proposed in this paper reduces THD upto 1%. The simulations are done in MATLAB simulink and comparative results of THD for different firing angles are recorded.

Keyword: Converter, Harmonics, Pulse doubling ,THD

I. INTRODUCTION

In the past few decades, researches are going on to increase the quality of power supplied by utility. Due to improvements in the field of power electronics, effective conversion of AC to DC can be done by semiconductor devices like diode, thyristors, IGBT etc. Six pulse converter has been used widely for AC-DC/DC-AC conversion. Six pulse converter can eliminate harmonics content in input current only upto 3rd level, i.e , the harmonic distortion is more in six pulse converter. Researchers found that as the pulse number is increased, the harmonic distortion is decreased. Thus a method of increasing pulse number was found out by increasing the number of converter circuit. The cost of semiconductor devices is high and therefore the cost of converter circuit also increases as the number of pulses increase. Thus 12 pulse converter is being used in industries as it cancels harmonic upto 11th level and the distortion is satisfactory. But the percentage of total harmonic distortion does not meet the IEEE standard of 5%. In order to achieve this, the pulse number is to be increased. The method of increasing number of converter circuit will lead to high cost of converter circuit and therefore researches are going on to find an alternative method.

Multipulse converters have various applications like hydroelectric, gas turbine, diesel, biomass and wind system based power plants. The renewable energy systems need converter system to control the power output as the source for power plant is not continuous and steady. The use of semiconductor switches in the converter produce harmonic distortions. But the power produced is desired to have less harmonic content as possible. The use of 24 pulse converter can eliminate harmonics upto 21st level in the input line current, which can meet the IEEE standard.

The proposed 24 pulse converter is developed through pulse doubling technique in 12 pulse converter circuit. Thus, the existing 12 pulse converter can be easily replaced by the proposed circuit without much alterations. 12 pulse converter is achieved by cascading two six pulse converters in series or parallel. The converters should be 30° phase shifted from each other to attain 12 pulse output. 24 pulse can be achieved in the same method by cascading four 6 pulse converters which are 15° phase shifted to each other. In the proposed 24 pulse converter only 2 set of six pulse converter is required. Figure 1 shows the schematic diagram of the existing 12 pulse converter. ZSBT (zero sequence blocking transformer) and interphase reactor is used for attaining pulse doubling characteristics in the circuit.

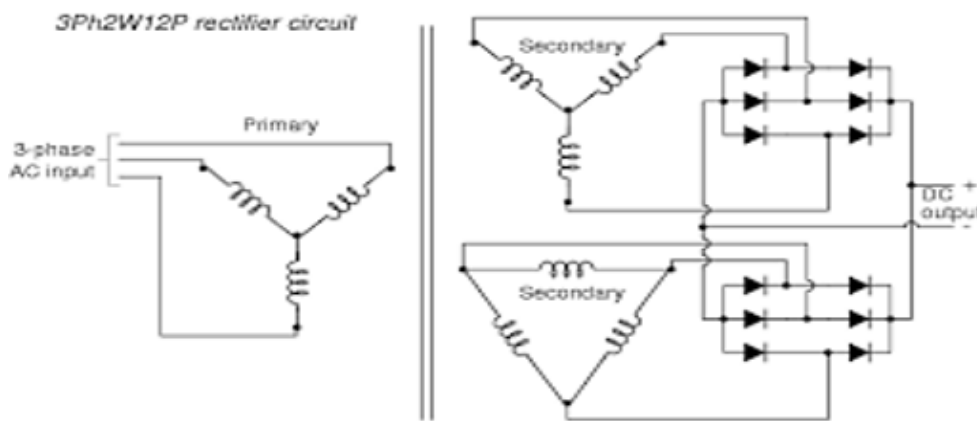


Figure 1: Image showing existing 12 pulse converter

II. MULTIPULSE CONVERTERS

A converter whose pulse number is greater than six is categorized as multipulse converters. Assuming three phase supply, the minimum pulse number under this category is twelve and that converter is named as 12 pulse converter. The number of pulses can be increased as multiple of 6 like 12, 18, 24, 30, 36, 48 etc. The harmonic content in the input current mains corresponding to pulse number of converter is given in table 1. The minimum phase shift between each converter circuit is calculated as,

Phase shift = $60^\circ / \text{number of converter circuit used}$.

Multipulse converters are categorized as improved power quality AC-DC converters (IPQC) which are used in high power applications involving high voltage and low current. Multipulse converter reduces current harmonic content, improves power factor, increases efficiency, elimination/reduction of DC filters, reduced voltage distortion and well regulated DC output resulting in improvement in power quality.

TABLE 1: Table showing Variation Of Harmonics With Pulse Number

Pulse number	AC harmonics
1	1,2,3.....
2	1,3,5.....
3	2,4,5.....
6	5,7,11.....
12	11,13,23.....
18	17,19,35.....
24	23,25,47.....

III. 12 PULSE AC-DC CONVERTERS

12 pulse rectifier is the combination of two 6 pulse rectifier in cascaded form. The phase shift of 30° is required to produce 12 pulse rectification. It is achieved through three winding transformer. The primary of the transformer is in star connection where as one of the secondary is star connected and the other secondary is delta connected. Thus the delta connected winding produces a 30° phase shift. The converter 1 is connected to star connected secondary and converter 2 is connected to delta connected secondary. Figure 2 shows the simulation diagram of 12 pulse converter. The output of the rectifier contains 12 pulses which is shown in figure 3. The THD analysis of 12 pulse converter is shown in figure 4. The magnitude of output voltage,

$$V_0 = V_{01} + V_{02}$$

Where V_{01} and V_{02} are output voltages of converter 1 and converter 2 respectively.

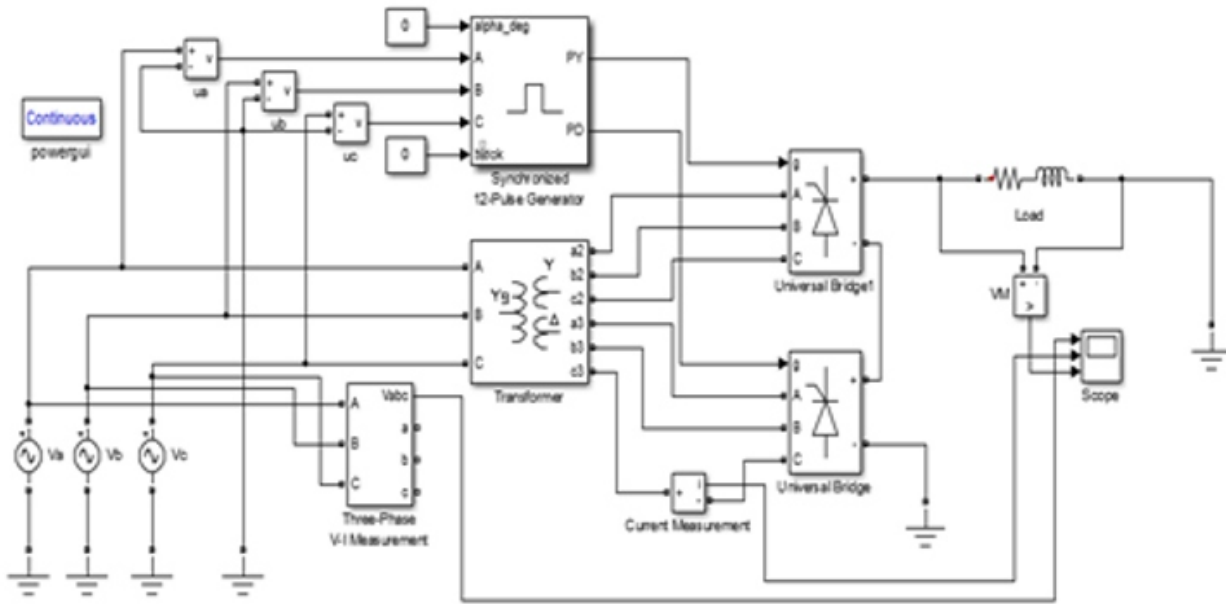


Figure 2: Image showing simulation of 12 pulse converter

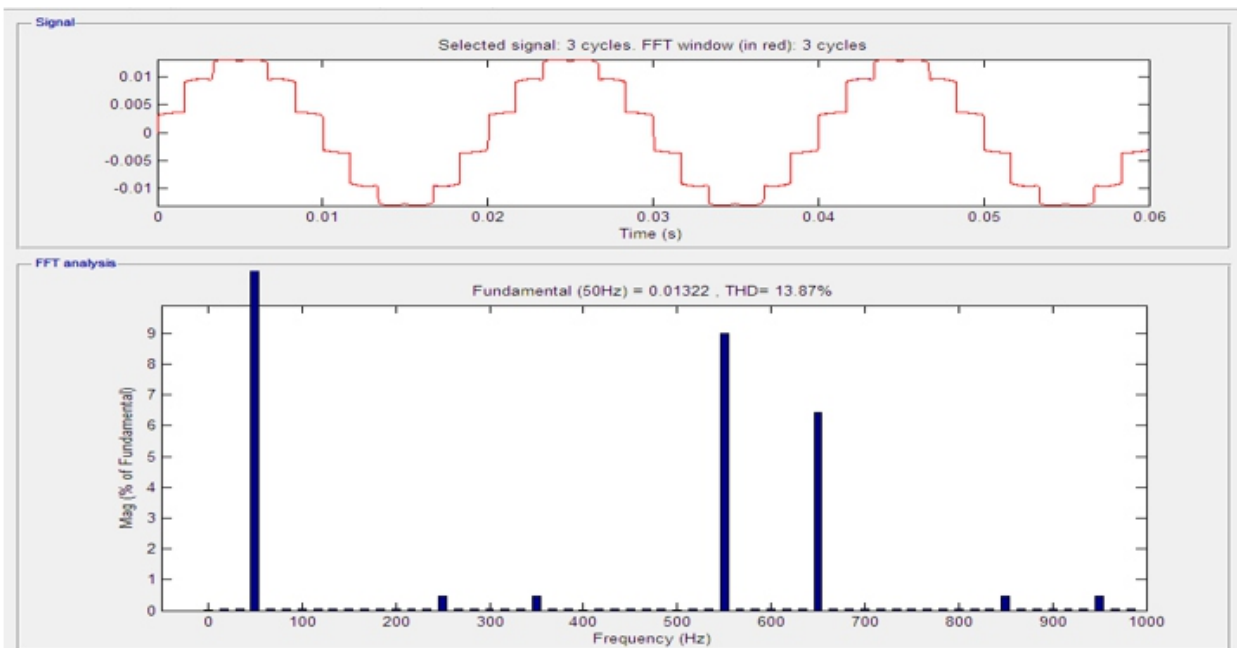


Figure 4: Image showing THD analysis of 12 pulse converter

IV. PROPOSED 24 PULSE CONVERTER

Figure 5 shows the block diagram of proposed 24 pulse converter. In the existing 12 pulse converter, if inter phase reactor (IPR) of proper design is added then the output will be 24 pulse converter. Inter phase reactor is being used in industries so as to draw near sinusoidal current from utility. By proper design of IPR, the THD value can be brought nearly 1 %.

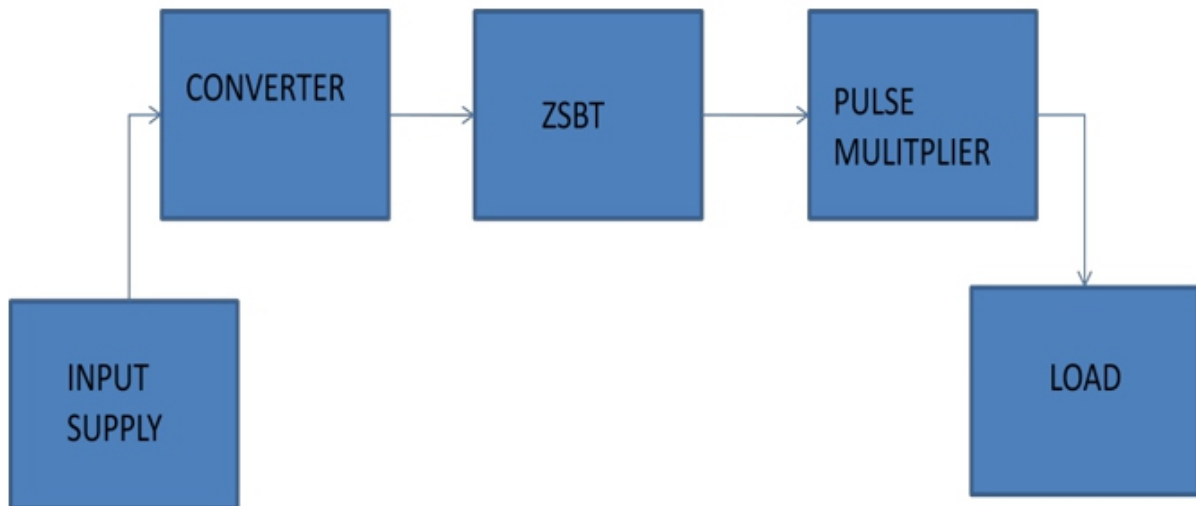


Figure 5: Image showing Block Diagram of Proposed 24 Pulse Converter

Figure 6 shows the schematic diagram of proposed 24 pulse converter. Zero sequence blocking transformer is used to attain the following :

- (a) Independent working of the two converter circuit.
- (b) To block zero sequence current as it does not cancelled out as it is in phase in the output of two converters.

The two diodes tapped from IPR will on/off according to the voltage difference to produce 24 pulse output.

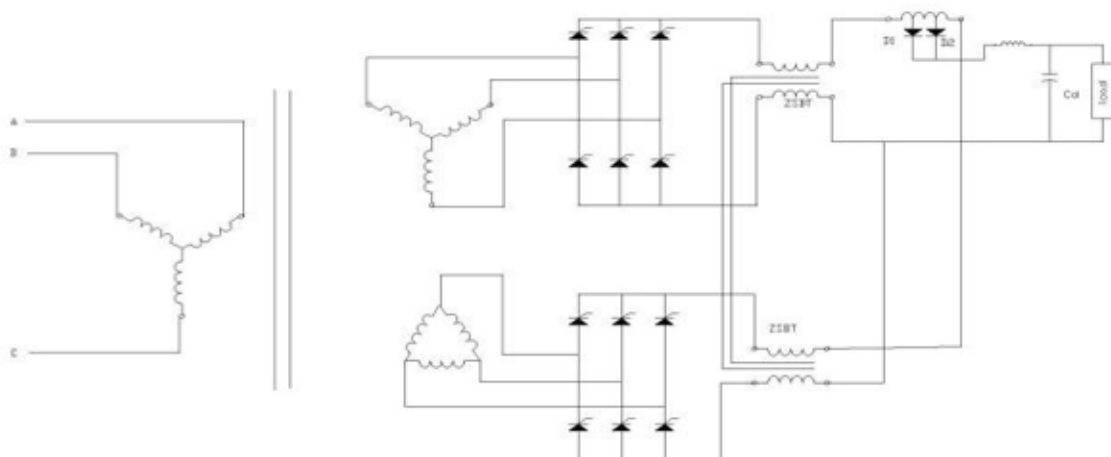


Figure 6: Image showing Schematic of Proposed 24 Pulse Converter

A. DESIGN OF INTER PHASE REACTOR

Inter phase reactor (IPR) not only ensures smooth current flow, if properly designed produces pulse doubling. Here 3 winding reactor is used in which the end most windings have turns equal to half the number of turns of the middle winding. The diodes connected get on/ off respective to the voltage across the windings of reactor to produce pulse doubling from where the diodes are tapped.. The frequency of the voltage appearing across the IPR is 6 times the source frequency. The diodes conducts according to the polarity of the voltage across the reactor windings. The turns ratio os the reactor windings is given by

$$N_A/N_0 = 0.2457$$

B. DESIGN OF ZSBT

Zero sequence blocking transformer is connected at the output of the two rectifiers in order to achieve independent operation of the converter circuits. The zero sequence component of the voltage and current present in the output of the two converters will not cancel out with each other as they are in phase. ZSBT blocks the zero sequence component present in the DC output. The voltage appearing across the ZSBT contains triplen frequency components and therefore ZSBT can be of small size, weight and volume. Thus the retrofitting application of 24 pulse converter can be done cost effectively. The design of ZSBT can be calculated in the same way as IPR.

V. MATLAB SIMULATIONS AND RESULTS

The proposed 24 pulse converter and the existing 12 pulse converter is simulated in MATLAB simulink using PSB toolboxes. Figure 7 shows the simulation circuit of 24 pulse converter. Figure 8 shows the output waveform and THD analysis of 00 firing angle. Figure 10 shows output waveform and THD analysis for 00 firing angle. Table 2 shows the variation of THD with different firing angles.

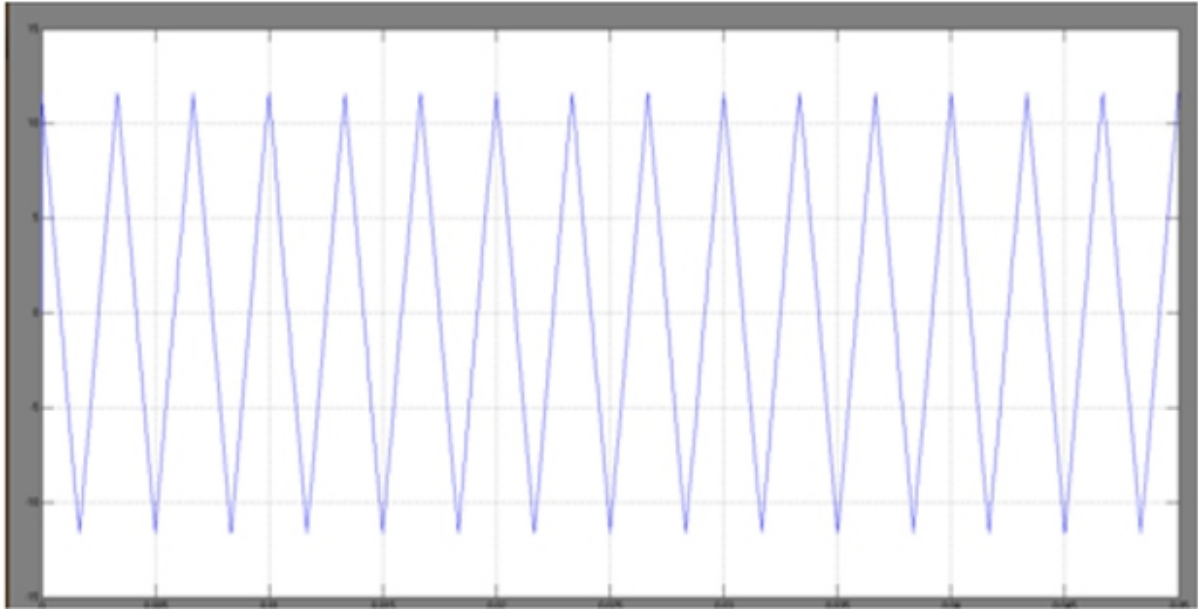


Figure 10: Image showing Voltage waveform across IPR

TABLE 2: Table showing Comparison of THD With Different Firing Angles

Firing angle (degree)	THD (percentage)
0	1.03
20	1.97
40	2.6
90	4.68

VI. CONCLUSION

The proposed 24 pulse converter is simulated in MATLAB simulink and the output for different firing angles has been recorded. Replacement of existing 12 pulse converter can be done cost effectively using the proposed converter as the pulse multiplier circuit used is of small ratings, weight and volume. The proposed circuit can be done using IGBT for high voltage applications.

VII. REFERENCES

- [1] Abhay Chaturvedi and Deepika Masand “Comparative Analysis of Three Phase AC-DC Controlled Multi Pulse Converter”, *IEEE Transaction*, SCEECS 2012.
- [2] Ages.J and Silva.A, 'Analysis and Performance of A 12-pulse High Power Regulator', *Conf. Rec. Power Modulator Symposium 1994*, pp. 156-158.
- [3] Chaturvedi P.K., et al., “Multi-Pulse Converters as A Viable Solution for Power Quality Improvement” June 2006.
- [4] Choi .S, et al., 'New 24-pulse diode rectifier systems for utility interface of high power ac motor drives', *IEEE Trans. on Industry Applications*, Vol. 33, No. 2, March/April.1997, pp. 531- 541.
- [5] Hahn Jaehong, et al., 'Analysis and design of harmonic subtracters for three phase rectifier equipment to meet harmonic compliance', *Proc. IEEE, APEC '00, Feb. 2000, Vol. 1*, pp. 211-217.
- [6] Kamath G. R., et al., 'A compact autotransformer based 12-pulse rectifier circuit', in *Proc. 2001, IEEE IECON, Conf.*, pp. 1344-1349.
- [7] Paice D. A., *Power Electronic Converter Harmonics: Multipulse Methods for Clean Power*, New York, IEEE Press 1996.
- [8] Scaini Xince P Eng, Bruce m. vrbn PE, ”Proposed Multi-pulse Converters & Their Operational Benefits”, *IEEE p.p. PCIC 98-19*.
- [9] Shota Miyairi, Shoji Iida, Kiyoshi Nakata & Shideo Masukawa, 'New method for reducing harmonics involved in input and output of rectifier with interhase transformer', *IEEE Trans. on Industry Applications*, Vol. 22, No. 5, Oct./Nov.1986, pp. 790-797.
- [10] Villablanca M.E. & Arrilaga J.A., 'Pulse multiplication in parallel converters by multi tap control of interphase reactor', *IEE Proceeding-B*, Vol. 139, No. 1, Jan. 1992, pp. 13-20.
- [11] Yeddo B Blauth and IVO Barbi, “A Phase Controlled Twelve Pulse Rectifier without Phase Shifting Transformer”, *IEEE Transaction*, p.p.-7803, September 1998

Series Combination Of Hybrid Filter With Distorted Source Voltage

¹S. Dineshkumar,

¹Assistant Professor - Department Of Eee, M. Kumarasamy College Of Engineering,
Thalavapalayam, Karur, India.

ABSTRACT

The use of power electronic devices in industry and domestic applications such as adjustable speed drives, inverters, furnaces, computer applications and other electronics devices let to the injection of harmonics and reactive power in the power system. So harmonic filter is important one for filtering harmonics in the power system. The shunt active and shunt passive filter is designed for compensating 5th and 7th harmonics. Hybrid filter performance was verified through MATLAB/SIMULINK where the source voltage having 3rd harmonic component. Thus the hybrid filter provides an effective harmonic compensation and reactive power compensation.

Keywords—Hybrid power filter, nonideal mains voltage

I. INTRODUCTION

The power electronic devices are used for ac power control in the power system. The harmonics injection and reactive power cause disturbance to the customer and interference in the communication line with low system efficiency and poor power factor. Many researchers have provided solutions for harmonic and reactive power compensation [1] and they imposed specific limitations of current harmonics and voltage notches. Passive filter is used for eliminating lower order harmonics and capacitors used for compensating reactive power demand in the system. They have some drawback such as fixed compensation and resonance problems. Then the fundamental frequency reactive power may affect the system voltage regulation.

Here the increased harmonic pollution leads to the development of active filters. The active filter rating depends on harmonics and reactive power to be compensated. Generally active filters required high current rating and higher bandwidth requirement that do not constitute cost effective solution for harmonic mitigation[7].

Hybrid filter with series combination of shunt active and shunt passive filter can overcome the demerits of active and passive filter [2]. The hybrid topology with series combination of active and passive filter reduces the rating of active filter, improves the filtering characteristic of passive filter and greatly reduces the precise tuning of passive filter. It supplies reactive power as per demand and maintains voltage regulation.

Many control strategies, starting from instantaneous reactive power compensation, evolved since the inception of shunt active filters. One of the control strategy based on DC link voltage was discussed [4] [5]. In this method the shunt active filter is to compensate the load side harmonics and reactive power, thereby making the load linear.

Therefore the supply side distortions are imposed on the line current. Even though this method meets the reactive power requirement of the load when the supply voltage distortion occur and the same are imposed on the line current also, where the line current still remains non-sinusoidal even after compensation.

In this paper the instantaneous reactive power algorithm has been used for shunt active filter with some modification that can effectively compensates the harmonics caused by source side distortion also. This proposed method overcomes this drawback by preprocessing supply voltage using park's transformation for that we are using only the fundamental positive sequence component of source voltage for reference current calculation.

Control block diagram and operational principles are discussed below. This proposed method can effectively compensate the harmonics and reactive power even when the source voltage is unbalanced.

II. CONTROL STRATEGY

Most of the active filters are designed based on the instantaneous reactive power algorithm. The instantaneous reactive power algorithm is derived based on the dq0 transformation, where they can calculate the current compensation based on a two-axis system [6]. In this method, the voltage and load current were first transformed into two- axis representation.

The instantaneous real and instantaneous reactive power consumed by the loads was calculated based on this representation system[3]. After compensation, the post compensated current in the two-axis system was required to inversely transform back to the three phase system from the grid; from this the reference signals of compensation current can be obtained.

$$I_a^* = I_m^* \sin(\omega t)$$

$$I_b^* = I_m^* \sin(\omega t - 120^\circ)$$

$$I_c^* = I_m^* \sin(\omega t - 240^\circ)$$

The control strategy proposed here is for making the compensated line current to be sinusoidal and balanced [7]. Therefore the objective includes a sinusoidal reference current calculation and the current control technique for generation of switching pulses to the VSI for a sinusoidal and balanced line current. Where I_m^* is the amplitude of the desired line current, the phase and frequency of the line current are obtained from the supply voltage. The magnitude of reference line current can get by regulating the DC bus voltage of VSI. The DC-link capacitance of VSI is used as an energy storage element in the system.

For a lossless active filter in the steady state, the real power supply from the supply should be equal to the real load demanded, and no more real power passes through the power converter into the capacitor. Therefore the averaged dc-capacitor voltage can be maintained at the reference voltage level. For a balanced line current under unbalanced source voltage the proposed method to use one phase of source voltage as phase reference and 120 shifter. By this method the harmonics present in the source voltage are reflected in the reference line current. Therefore, a modified algorithm, by preprocessing the source voltage template is proposed to make the compensated the line current sinusoidal.

The source voltages are transformed into d-q reference frame using park's transformation. After transformation nth order positive sequence component becomes $(n-1)^{\text{th}}$ order component becomes $(n-1)^{\text{th}}$ order component and nth order component becomes $(n+1)^{\text{th}}$ order component in d-q reference frame. The fundamental component of source voltage becomes a dc component in d-q reference frame which should be filtered out using a low-pass filter. This filtered dc value after counter transformation into 3-phase component can be used for unit templates for reference current calculation. Thus this modification filters out the effect of source side distortion in the line current.

In order to drive the line currents to trace the reference currents an effective current control technique has to be used for generating the switching pulses of the VSI. Hysteresis control is implemented here for this purpose. In this control line currents are sensed and compared with the reference currents. The error in each phase is sent to the hysteresis control, Where in a switching pulse is generated to the upper switch of the VSI, if this error is less than the lower hysteresis band and a switching pulse is generated to the lower switch of the VSI if the error is found more than the upper hysteresis band.

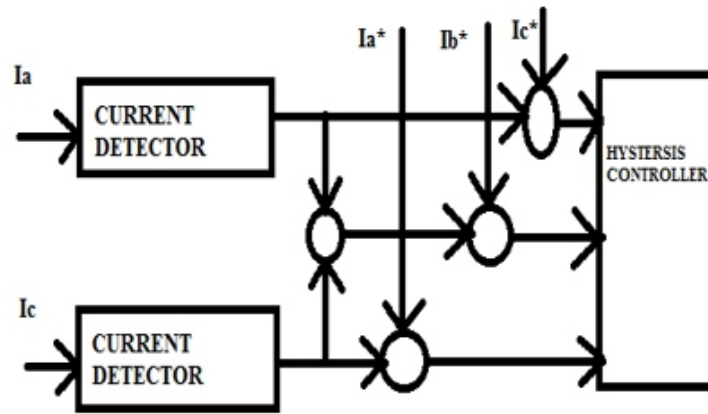


Fig1.1 Block diagram for control strategy

III. PROPOSED METHOD

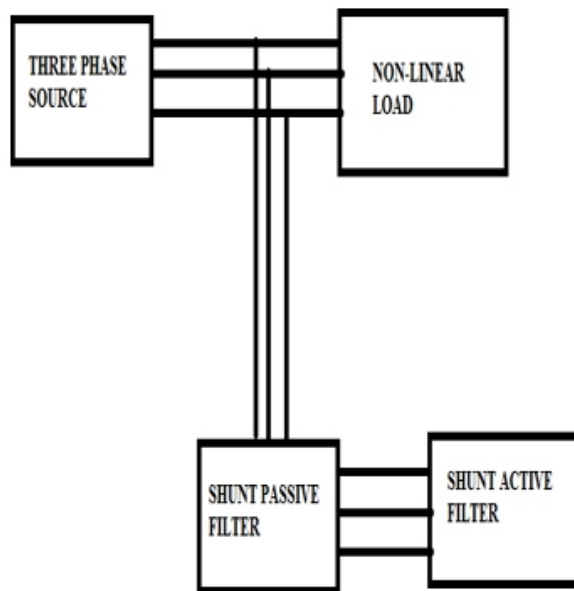


Fig1.2 Block diagram for series combination of shunt active and passive filters

The fig1.2 represents three-phase source and non-linear load. Where the shunt passive filter and shunt active filter are connected in series with the line. Passive filter provides cost effective mitigation for harmonics and reactive power from supply. Active filter can effectively compensate the harmonics and can meet the reactive power demand.

The hybrid filter with series combination of active filter and passive filter reduces the rating of active filter, which also improves the filtering characteristics and reduces the precise tuning of passive filter.

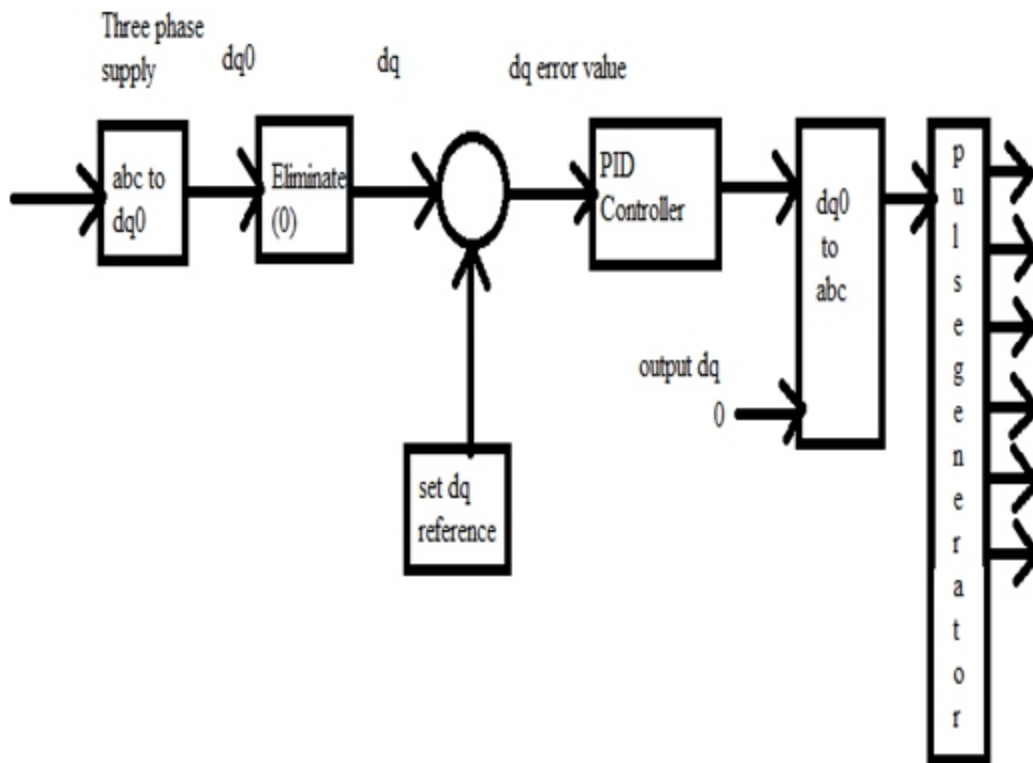


Fig1.3 Block diagram for controller

The fig1.3 represents the controller block diagram. Where three phase supply from the grid and they are converted into dq0 transformation. By eliminating the 0th term we get dq alone, setting dq reference value by comparing the actual value and reference value we get dq error value. PID controller output depends on the erroneous value. Then converting dq0 to abc value they are given as input to the pulse generator, by varying the amplitude can generate six pulse and given as input to the three-phase inverter.

IV. SIMULATION RESULTS

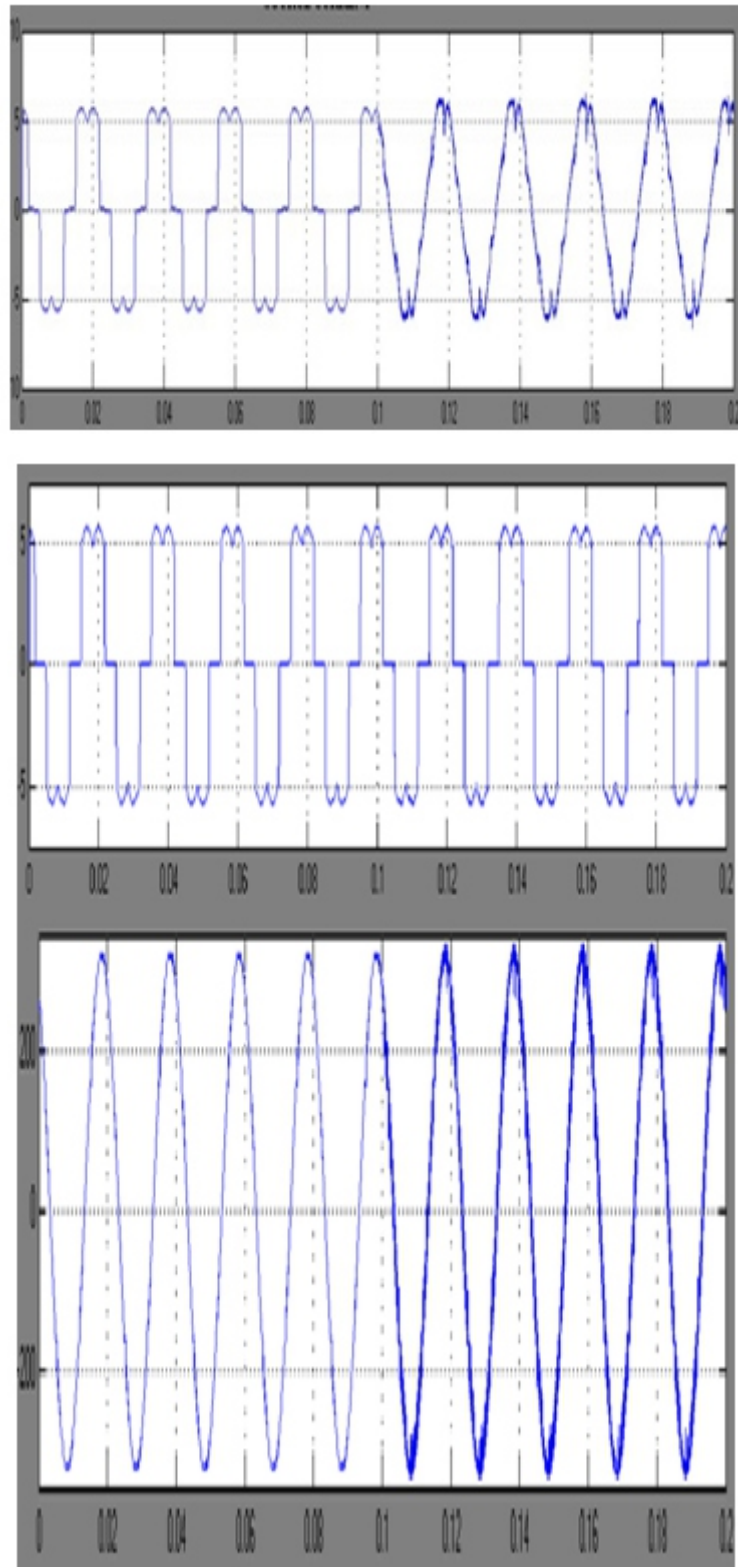


Fig 1.4 simulation result for series combination of hybrid filter

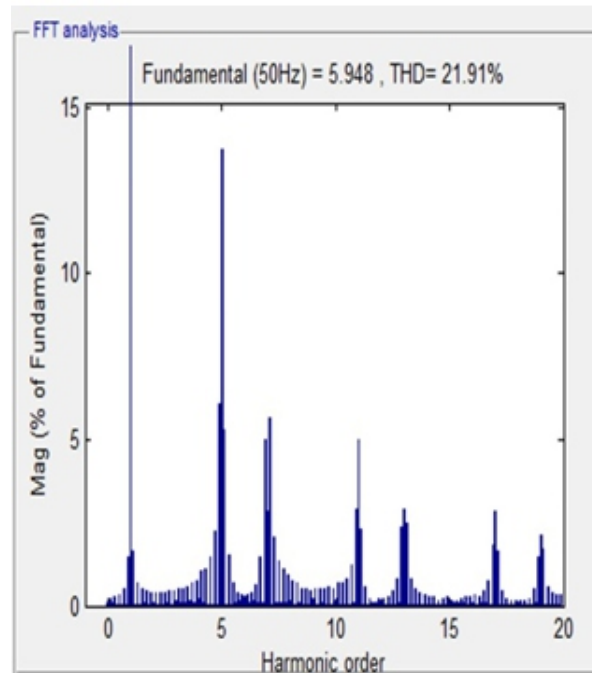


Fig 1.5 FFT analysis for hybrid filter in series combination

	Source voltage(Vs)	Load current(I_{load})	Line current (I_{line})	Compensating current(I_c)
Series combination of hybrid filter	25.23	30.65	21.91	25.18

Table 1. TDD values for various parameters

	Reactive Power (KVAR)	Filter Inductance (mH)	Filter Capacitance (μ F)
5 th harmonics (Q=40)	0.5	40	10
7 th harmonics (Q=40)	0.5	20.4	10
11 th harmonics (Q=50)	1	4.2	20

Table 2. Passive filter parameters

The active filter parameters are $L_c=3.35\text{mH}$, $R_c=0.4$ Ohms, DC-link capacitance $C_{DC}= 2200\mu\text{F}$, DC-link reference voltage $V_{dc,ref}=400\text{Volts}$ for series Hybrid filter topology.

Fig1.3 shows the simulation results for series combination of passive and active filter. The source voltage (Vs) is having a THD of 12.21%, and the load current (I_{load}) having a THD of 21.91%. The line current(I_s) after compensation is having 7.33%. The peak value of supply current is found less than the peak value of load current that shows the supply current is carrying only the active component of load current and active component of compensating current. The DC-link voltage of the VSI is maintained at 400Volts.

To drive the line currents to trace the reference currents an effective current control technique has to be used for generating the switching pulses for the VSI. Hysteresis control is implemented for this purpose. In this control the line current are compared and sensed with the reference current. Therefore this modification filters out the effect of source side distortions in the line current.

The topology of hybrid filters are simulated using MATLAB/SIMULINK and the results are compared under non-ideal supply voltage with a 0.1 pu 3rdm harmonic negative sequence component in the source voltage. The rms value of the fundamental component is 230Volts. The various design values of passive filter are shown in Table2.

V. CONCLUSION

The results show the use of hybrid filter topology for harmonic and reactive power compensation. However, hybrid filter topology with a series combination of active and passive filters is installed in place of an already existing passive filter, to make efficient. The passive filter performance might have affected due to changes in the system parameters. This topology helps in improving the performance of passive filter and the active filter can be used at a lower rating. In this paper, a new algorithm has been proposed to improve the active filter performance under nonideal main voltages. The performance of control strategy used here is simple and effectively compensates the load generated harmonics and nullifies the effect of source voltage harmonics in the line.

VI. REFERENCES

- [1].Bhim Singh, Kamal Al-Haddad and Ambrish Chandra," A Review of Active Filters for Power Quality Improvement"IEEE VOL.46,NO.5,OCT 1999.
- [2].Bhim Singh and Vishal Verma," An Indirect Current Control of Hybrid Power Filter for Varying Loads"IEEE VOL.21,NO.1,JAN 2006.
- [3]. Adil M. Al-Zamil and David A. Torrey," A Passive Series, Active Shunt Filter for High Power Applications"IEEE VOL.16,NO.1,JAN 2001.
- [4].Shyh-Jier Huang and Jinn-Chang Wu," A Control Algorithm for Three-Phase Three- Wired Active Power Filters Under Non ideal Mains Voltages" IEEE VOL.14,NO.4,JULY 1999.
- [5].Shailendra Kumar Jain, Pramod Agarwal and H. O. Gupta" A Control Algorithm for Compensation of Customer-Generated Harmonics and Reactive Power"IEEE VOL.19,NO.1 JAN 2004.
- [6]. Montero, M.I.M. , Cadaval, E.R. , Gonzalez, F.B. "Comparison of Control Strategies for Shunt Active Power Filters in Three-Phase Four-Wire Systems" IEEE VOL.18,NO.3 JAN 2005.
- [7]. Dineshkumar,S and Senthilnathan.N "Three Phase Shunt Active Filter Interfacing Renewable Energysource With Power Grid",IEEE Transactions on Communication Systems and Network Technologies (CSNT), pp. 1026-1031,2014.

Power Efficiency Improvement Method For A BI- Directional Dual Active Bridge DC-DC Converter

K. Divya,

Assistant Professor-Department of Electrical Engineering, M. Kumarasamy College of Engineering, Karur, India.

ABSTRACT

Bidirectional DC-DC converters, which makes possible the bidirectional transmission of power, have become indispensable in recent years, due to the diversification of the power supply network, including the use of batteries. Of these, the dual active bridge (DAB) DC-DC converter features a simple mechanism and symmetric circuit architecture making possible the equal transmission of power in both directions. Because of these advantageous characteristics, DAB DC-DC converters are in wide use. However, this circuit has the intrinsic problems that during light load conditions, switching surges occur and power efficiency decreases. This paper proposes digitally- controlled operation as a new method to resolve these problem.

Keywords- DAB, Pulse Width Modulation, Photo Voltaic.

I. INTRODUCTION

Recently, bidirectional dc–dc converters have been a focus of attention because of the huge demand for diversification of the power supply network, which includes the use of batteries. The dual active bridge (DAB) dc–dc converter is one of the most popular circuits for bidirectional applications because of its simple structure. Such applications include uninterruptible power systems [1], automotive [2]– [4], and energy storage systems [5]. One of the most important features of DAB dc–dc converters is the achievement of Zero Volt Switching (ZVS) in natural operation.

However, there are intrinsic problems with hard switching and/or power efficiency during light-load conditions [6]. Some research has been done to resolve these problems. For instance, the intrinsic topology of DAB converters has been examined closely, and by operating the input bridge in phase-shifted mode, with the output bridge running as an uncontrolled rectifier, the operating range for soft switching has been made wider. However, during light load, soft switching is limited to only part of this

extended range [7]. It was predicted that, through the use of Sic devices, there would be high efficiency, but during light load, there is the problem of lowered efficiency due to snubber condenser short-circuiting. Within high-density design approaches, there are those that employ a resonant switching method to achieve high efficiency. However, the soft-switching range has not been clarified, and because a snubber condenser is added, during light load, there is a concern about lowered efficiency due to snubber condenser short-circuiting [9]. Furthermore, by applying switching modulation, DAB dc–dc converters work over a wide range of input voltage and load conditions. The objectives of switching modulation controls are to regulate voltage and satisfy load variation, to expand the soft-switching region, and to minimize total power losses. In addition, as an operation mode to improve efficiency during light load, the TCM method is used, but with this, it is necessary to calculate three parameters: the primary side duty ratio, the secondary-side duty ratio, and the phase difference between the primary and secondary sides, for which the computational process is complicated. However, it is sufficient to calculate two parameters: width and phase difference between the primary and secondary sides, for which the computational process is relatively simple.

This project proposes a simple solution for power efficiency improvement with digital operation. This method can improve power efficiency due to switching loss reduction without adding other circuits such as a snubber circuit.

II. EXISTING METHOD

It describes about the review of existing method problems also provides solution to these problems. The four power switches are used to achieve the goal of bidirectional current control and in this soft switching, synchronous rectification, voltage clamping are included to reduce switching and conduction loss caused by utilizing low voltage rated with small drain source resistance [1]. To improve the current stress problem during bidirectional power flow and to provide high voltage conversion ratio which includes the presence of saturation constraint for the magnetic design of resonant inductor lead to limitations in maximum output power and voltage conversion ratio [5]. The dual active bridge DC-DC converter uses high frequency AC link current as control parameter that control of parameters which are slowly varying by natural affects the system dynamic response [7]. When main power source is not able to meet peak power demand dynamic response should be improved. Dual half bridge topology is developed to achieve higher power rating using minimum number of device. ZVS is achieved in either direction of the power flow without voltage clamping circuit and resonant components by defining dead time of gate pulses and so in this soft switching can be inferred in buck mode and also the current stress is proportional to phase shift angle [3]. Achieving bidirectional power flow for battery charging and

discharging using only one transformer with the help of high frequency and half bridge in the primary and current fed push pull on the secondary side which has current control mode that is used for both modes of converter operation [4]. Thus these various disadvantages that have occurred in the previous projects that have overcome by using the high frequency transformer for the power efficiency improvement technique.

III. PROPOSED METHOD

3.1. BLOCK DIAGRAM

From the solar panel input is given to the system. Solar panel consists of PV cells. The number of PV cells used depends upon the needed voltage. Fig. 1 illustrates the block diagram of proposed method.

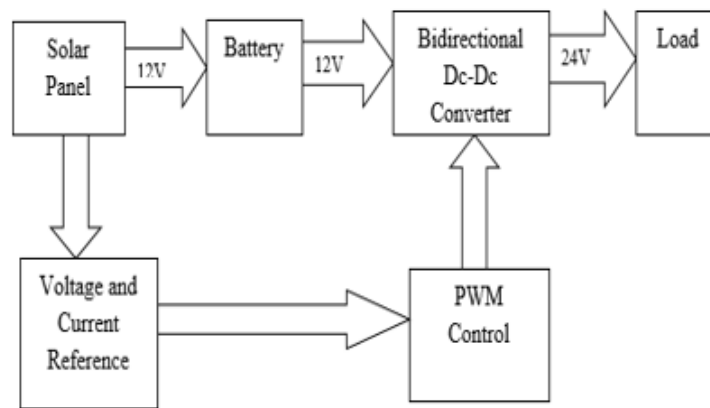


Figure 1-Block diagram of proposed method

A bi-directional converter can move power in either direction, which is useful in applications requiring regenerative braking. In these DC to DC converters, energy is periodically stored into and released from a magnetic field in an inductor or a transformer, typically in the range from 300 KHz to 10 MHz. By adjusting the duty cycle of the charging voltage (that is, the ratio of on/off time), the amount of power transferred can be controlled. Pulse-width modulation (PWM), or pulse-duration modulation (PDM), is a commonly used technique for controlling power to inertial electrical devices, made practical by modern electronic power switches. The average value of voltage (and current) fed to the load is controlled by turning the switch between supply and load on and off at a fast pace. The longer the switch is on compared to the off periods, the higher the power supplied to the load.

3.2. CIRCUIT DIAGRAM

The circuit diagram consists of solar panel, battery, inverter, rectifier, controller, comparator, ferrite core transformer, optocoupler, DC motor. The solar panel produces an output of 12V, which is stored in the battery. The forward biased diode is placed between battery and PV panel because to save PV panel from reverse flow of current from battery to PV panel. The power supply circuit is used to give constant voltage through voltage regulator IC7805. The output from power supply circuit is given to controller circuit. The comparator is used to compare PV output voltage and inverter input voltage, and the resultant voltage is given to the controller.

The controller gives the gating signal to the inverter and rectifier circuit. The output DC voltage 24V is fed to the DC series motor.

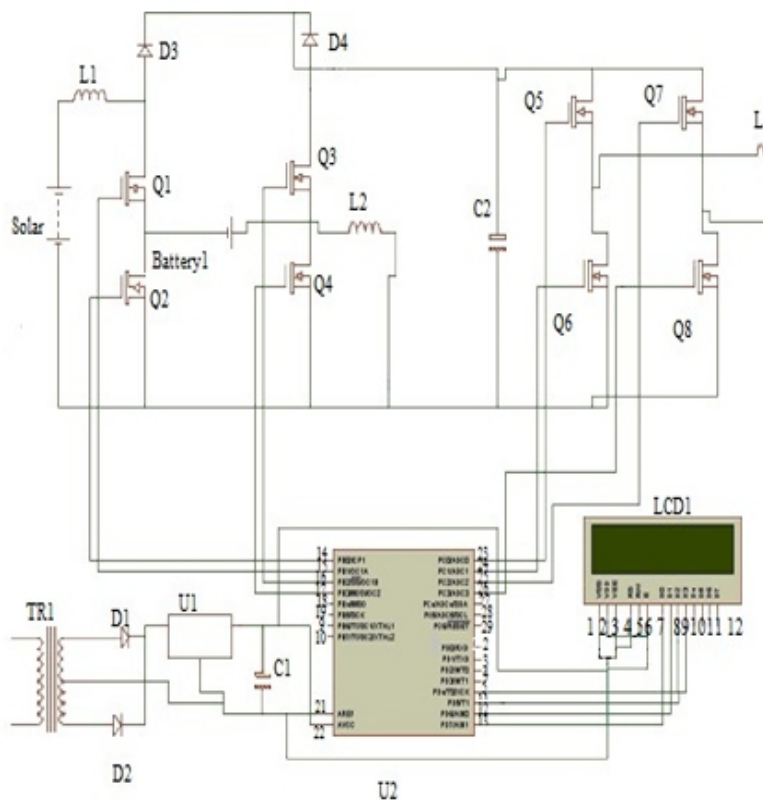


Figure 2-circuit diagram of proposed method

Figure.2 illustrates the circuit diagram of proposed method. The converter used is bidirectional converter so reverse operation is also possible. Input from the supply is given to the step down transformer and it is given to the bridge rectifier which converts AC into DC and the inverter circuit converts DC into pulsed AC. The rectifier circuit again converts AC into DC supply which gets stored in the battery.

IV. RESULT AND DISCUSSION

4.1 SIMULATION RESULT

The simulation is done by MATLAB software. The output generated from solar panel is taken as reference and is compared with rectifier output and with the compared value the microcontroller will generate PWM signal. The generated PWM signal is given to the MOSFET switches. The converter used is bidirectional converter so reverse operation is also possible. Input from the supply is given to the transformer and it is given to the bridge rectifier which converts AC into DC and the inverter circuit converts DC into pulsed AC. The rectifier circuit again converts AC into DC supply which gets stored in the battery. By using this bidirectional dual active bridge DC-DC converter, power efficiency is improved. When comparing with other converters efficiency of this converter is quite high. The simulation results can be verified by using the MATLAB software. Solar panel gives 12v supply to the dual active bridge DC-DC converter. Eight MOSFET switches are used. Discrete pulse width modulation is used for giving gate signal to the switches.

First four MOSFET switches act as inverter which converts DC supply into AC supply. The next four MOSFET switches act as a rectifier and converts AC supply into DC supply and it is given to the load.

The resonant inductor present in both sides of the transformer will boost up the supply when it is flow from source to load and buck the supply when it is flow from load to source. While running the simulation result power efficiency is improved upto 98% which is shown in the display.

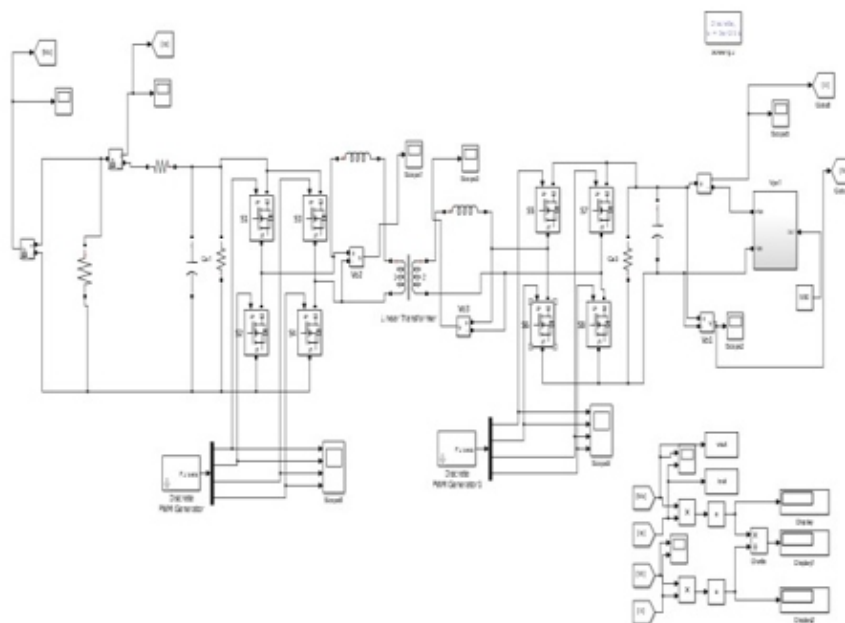


Figure 2- Simulink diagram of proposed method

The modulation index which depends upon the on and off time. Then by varying the duty cycle value the output of the converter can be changed.

In simulation the constant value of 250 is given to solar panel which denotes the luminous intensity. The luminous intensity value ranges from 250 to 750. Depending upon this value the output voltage varies. It produces output of 12V which is given as input to battery. Battery in turn gives it to Converter Bridge. Converter Bridge consists of four MOSFET switches which performs the operation of inverter and converts DC supply into AC supply.

Gating signal to this switch is given through pulse width modulation technique. Here discrete pulse width modulation is used. The resonant inductor present in both sides of transformer will responsible for buck mode and boost mode operation. When the power flows from source to load it will operate in boost mode and when it is flow from load to source it will operate in buck mode. During boost mode of operation in the positive half cycle the switches s1, s4, s5 and s8 are turned on then in the negative half cycle the switches s2, s3, s6 and s7 are turned on.

Hence the flow of current in boost mode is from source to load and in buck mode it is from load to source because during positive half cycle the switches s2, s3, s6 and s7 are turned on and in negative half cycle the switches s1, s4, s5 and s8 are turned on. The transformer used here is ferrite core transformer which will operate in high frequency around 1KHz. The efficiency of about 98% is obtained in boost mode and 96% is obtained in buck mode.

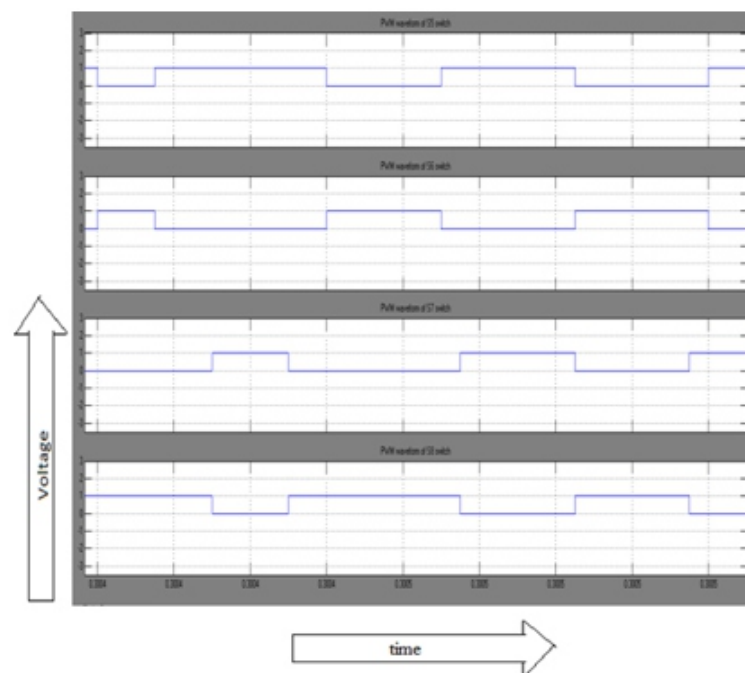


Figure 3-The Pulse Width Modulation for rectifier.

Figure 4 waveform shows about the Pulse Width Modulation for rectifier. The waveform obtained depends upon the pulse width. By varying the duty cycle, pulse width can be varied simultaneously.

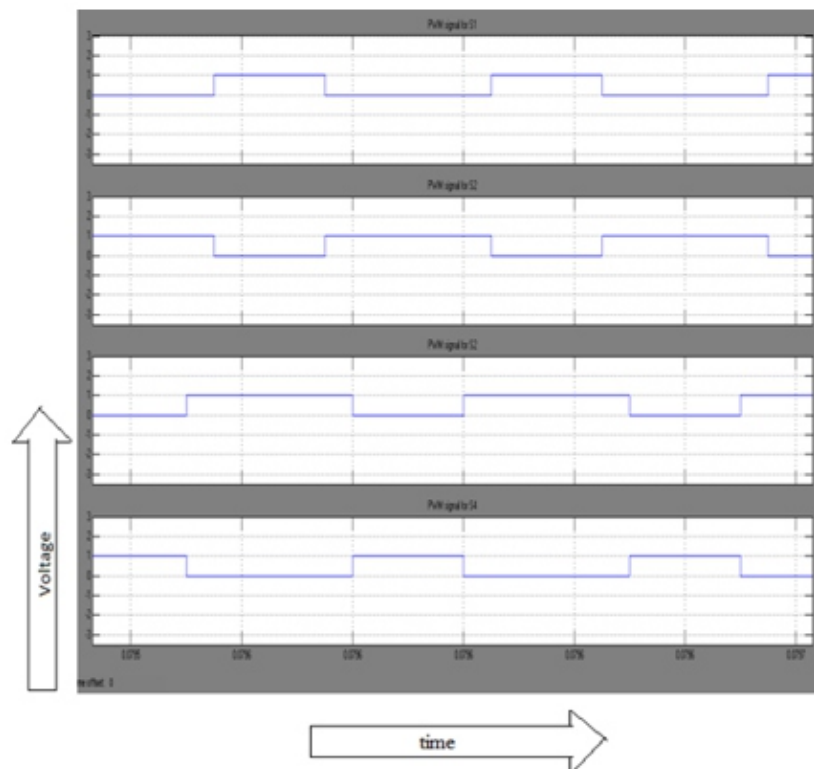


Figure 4-The Pulse Width Modulation for inverter.

Fig 5.3 shows about the Pulse Width Modulation for inverter. Depending upon the on and off time the duty cycle is varied accordingly. The operation of the converter depends upon the applied duty cycle. It is either inverter operation or rectifier operation.

If the duty cycle is above 50% then the converter performs boost operation. If it is less than 50% then the converter performs buck operation.

V. CONCLUSION

In this paper, energy is conserved by using renewable solar energy as input. Good static and dynamic response is obtained by the operation of dual active bridge DC-DC converter. Efficiency of other converters are low when compared with this proposed converter.

This converter implements ferrite core transformer. Hence core loss is very low and efficiency can be improved. Efficiency of this converter is improved upto 98% in simulation result. In future hybrid electric vehicle can be developed by implementing this converter model.

Through the analysis of the circuit operation and experimental results, it was possible to demonstrate the validity of the proposed operation for a DAB dc– dc converter. Applying the two modes, which is the proposed operation and conventional operation, the circuit can be operated over the full load range. The proposed operation method with digital operation can reduce switching surges without the addition of other circuits such as a snubber circuit.

From the experiment results, it could be confirmed that the surge voltage and surge current attributable to diode reverse recovery time that occur during light load are significantly reduced compared to conventional operation. Furthermore, due to the surge reduction method in the proposed operation, a maximum power efficiency improvement of 98% could be confirmed.

VI. REFERENCES

- [1] H. -J. Chiu and L. -W. Lin, "A bidirectional DC- DC converter for fuel cellelectric vehicle driving system," *IEEE Trans. Power Electronics.*, vol.21, pp.950-958, Jul. 2006.
- [2] R. W. A. A. De Doncker, D. M. Divan, and M. H. Kheraluwala, "A three-phase soft-switched high- power-density DC/DC converter for high-power applications," *IEEE Trans. Industry Applications*, vol.27, pp.63-73, Jan. /Feb. 1991.
- [3] T.Hirose, K.Nishimura, T. Kimura, and H. Matsuo, "An ac-link bidirectional DC-DC converter with synchronous rectifier," in *Proc.IECON 2010 36th Annual Conference on IEEE Industry Electronics Society*, pp. 351-357.
- [4] Gui-Jia Su, *Multilevel DC-Link Inverter*, VOL. 41, NO. 3, MAY/JUNE 2005.
- [5] S.Inoue and H. Akagi, "A bidirectional isolated DC-DC converter as a core circuit of the next- generation medium-voltage power conversion system," *IEEE Trans. power Electronics.*, vol.22, pp. 535-542, Mar.2007
- [6]M.H.Kheraluwala, R. W. Gascoigne, D. M. Divan, and E. D.Baumann, "Performance characterization of a high-power dual active bridge DC-to-DC converter," *IEEE Trans. Industry Applications*, vol.28, pp. 1294-1301, Nov. / Dec. 1992.*Single- Phase Multilevel Inverter Using Second- Order Switching Surface*, VOL. 24, NO. 10, OCTOBER 2009.
- [7]F.Krismer, and J. W. Kolar, "Accurate small- signal model for the digital control of an automotive bidirectional dual active bridge," *IEEE Trans. Power Electronics*, vol. 24, pp. 2756-2768, Dec. 2009.

Design Of Embedded System Based Rapid Sensing AC Electrical Capacitance Tomography

K. Manikandan, S. Sathiyamoorthy

¹Department of Electronics and Instrumentation Engineering,
J.J. College of Engineering and Technology, Anna University of Technology, Tiruchirappalli, India.

²Department of Electronics and Instrumentation Engineering, College of Engineering and
Technology, Tiruchirappalli, India.

ABSTRACT

An electrical capacitance tomography (ECT) sensor consists of eight electrodes, usually mounted outside on insulating pipe. The principle difficulties to predict the real time data from the ECT sensor are permittivity distribution between the plate and capacitance is nonlinear; the electric field is distorted by the material present and is also sensitive to measurement errors and noise. This paper describes rapid sensing an AC ECT system and interface has been developed with embedded system. The combinational electrodes are fast switching by programming in the embedded system. The development of new method of this system is to increase the measurement accuracy, signal processing speed and reduce the signal-to-noise ratio.

Keywords – Electrical Capacitance Tomography, Electrodes, Embedded System, Real Time System, Permittivity.

I. INTRODUCTION

An ECT sensor consists of multiple electrodes, usually mounted outside an insulating pipe, the capacitance measured from the multiple electrode sensors. The changes in capacitance based on the presence of permittivity distribution, which in turn maps the material distribution in the process [1]. ECT is one of the imaging techniques most likely to provide quantitative flow visualization flow rate information in industrial flows. It has particularly used in two-phase oil/gas and gas/solid flows typical of petroleum and process industry [3-5]. The ECT can be obtained the internal information is valuable for understanding complicated process, verifying computational fluid dynamic models, measurement and control can be compared with other industrial tomography models. ECT offer more advantages of rapid response, no radiation, non-intrusive and non-invasive, withstanding high temperature and pressure and low cost. This technique is also used for biomedical field applications instead of CT and X

-rays, because the ray has more radiation [6-8]. It has been used for many industrial applications such as gas, oil, water flows in wet gas separators, oil pipelines, pneumatic conveyors, cyclone separators and fluidized beds. This is used to oil field industries for monitoring the bubbles in oil flow based on the difference in their dielectric processes. In the fluidized beds, pharmaceutical industry is operated by trial and error, because of the lack of online measurement tools. The operation of the pharmaceutical fluidized beds cannot be optimized; the low operation efficiency and product quality cannot be guaranteed. ECT has been used in pharmaceutical fluidized beds successfully [9-12]. The technique is capable of monitoring, both continuously and simultaneously, the local and global dynamic behavior of the gas bubbles and the solid particles in a noninvasive manner. Electrical capacitance tomography (ECT) has prospective uses for applications to real chemical processes, since mostly they are using organic liquids, which are nonconductive, rather than widely used water as model liquid in laboratory [15].

In this paper, discusses about the voltage flow in the ECT system. The most commonly used data predicted from ECT system are micro processor or microcontroller based system. But the response time for the single measurement is approximately 10.4-m sec. the time to reconstruct one image was measured was to be approximately 8.48 msec. This paper describes an intelligent interface has been developed with vital role of embedded system. The in-homogeneity of sensors sensitivity distribution and medium distribution are fully considered. The sensor is designed and constructed based on ac triangle wave as input signal with 20 kHz. The sensitivity of the measurement is up to 0.3 femto farads the minimum speed of measurement is brought to 1500 frames per second.

2. PRINCIPLE OF AC ECT SYSTEM

The AC ECT system sensor is mounted equally around the cross-section of the pipe, with an earthed screen outside the electrode to reject external noise. The number and size of the capacitance electrodes used depends on the application. A larger number of electrodes will give a higher resolution image but the measurement sensitivity will be low. The sensitivity can be increased by using longer electrodes but this will lower the axial resolution. If high axial resolution is required, a small number of short electrodes can be used together with separately excited axial guard electrodes, which prevent the electric field from spreading excessively at each end of the sensor electrodes. The sensor with N-measuring electrodes, there are $N(N-1)/2$ electrode pairs and thus $N(N-1)/2$ independent capacitances are measured. These measurements for 8 electrodes are suitable, so the sensor is connected in excitation signal and suddenly started the current flow in the electrodes. The current flow is dependent on distance between two electrodes and permittivity of the medium inside the tube.

The parameters of ECT sensors can be summarized as follows [2]:

1. Thickness and the material of the wall between the electrodes and the sensing zone.
2. Thickness and the material of the wall between the electrodes and the screen.
3. Size of the electrodes.

While designing the electrodes, the electrodes the insulation lining between the electrodes is the greater importance. The area and distance between the plates are constant. In these technique the current values will detected in the system. It will depend on the permittivity value of the material located between the electrodes. The figure1 shows the block diagram AC ECT system.

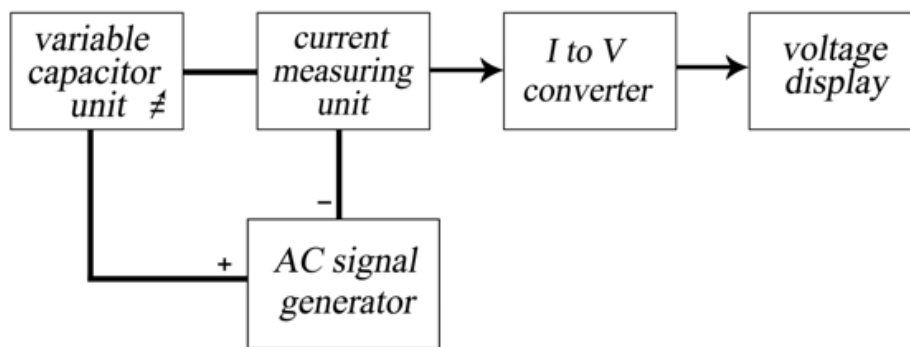


Figure 1. Block diagram of AC ECT system

3. METHODOLOGY

3.1. CAPACITANCE MEASUREMENT

The resolution of the ECT system depends upon the how fast the transducer senses the small change in capacitance with higher degree of accuracy and the number of electrode plates used in the system. The number of sensor electrodes that can be used depends on the range of values of inter-electrode capacitances and the upper and lower measurement limits of the capacitance measurement circuit. The pulse generator provides required excitation (pulse with well- defined fall and raise times) signal to the active differentiator capacitance transducer. At the output of the active differentiator a positive and a negative peak result. These peaks are separated using a peak-to-peak detector and are summed by a differential amplifier. The micro controller generates control signals to control of CMOS switches to select the excitation and detection electrodes, control of the multiplexer to select the DC signals, in turn, from the capacitance measuring circuit; and control the gain of the amplifier to make full use of the measurement range of the ADC and stores all the inter- electrode capacitances which will be used for image reconstruction. The time during which the capacitor charges from $1/3 V_{cc}$ to $2/3 V_{cc}$ is equal to

the time the output is high and is given by

$$T_C = 0.69(R_A + R_B) C \quad (1)$$

Similarly, the time during which the capacitor discharges from $2/3 V_{cc}$ to $1/3 V_{cc}$ is equal to the time the output is low and is given by

$$T_D = 0.69 R_B C \quad (2)$$

Thus the total period of the output waveform is

$$T = 0.69(R_A + 2 R_B) C \quad (3)$$

This in turn, gives frequency of oscillation as

$$F_o = 1/T = 1.45 / (R_A + 2R_B) C \quad (4)$$

Thus varying R_A , R_B and C can vary the frequency of the pulse generator. Varying R_A and C can vary the pulse width.

3.2. DESIGNING OF EMBEDDED SYSTEM FOR FAST SWITCHING

The word 'tomography' represents image slicing. The image is obtained by rotating the detector and the source in such a way that points outside the plane give a blurred image.

Electrical capacitance tomography is a very high-speed technique to capture the real time data of the turbulent fluctuation in the flow field. So the charging and discharging of the electrodes are should be fast, which can be done by CMOS switches. The CMOS switches should be controlled fast, that can be done by the micro controller. When a pair of electrodes is selected, one of them is known as the active electrode is continuously charged and discharged by the multiplexer's switches. The active electrode is charged to voltage V_c , and to the input of the current detector potential via the multiplexer's switches. The micro controller controlled the selection of the source electrode and the detecting electrode. The microcontroller ports can control the 0 and 1 pins in the multiplexers. The two ports from the micro controller are used for this purpose. The micro controller sends the control signals to the multiplexers at the micro second ranges. The design of driving circuit is shown in figure2.

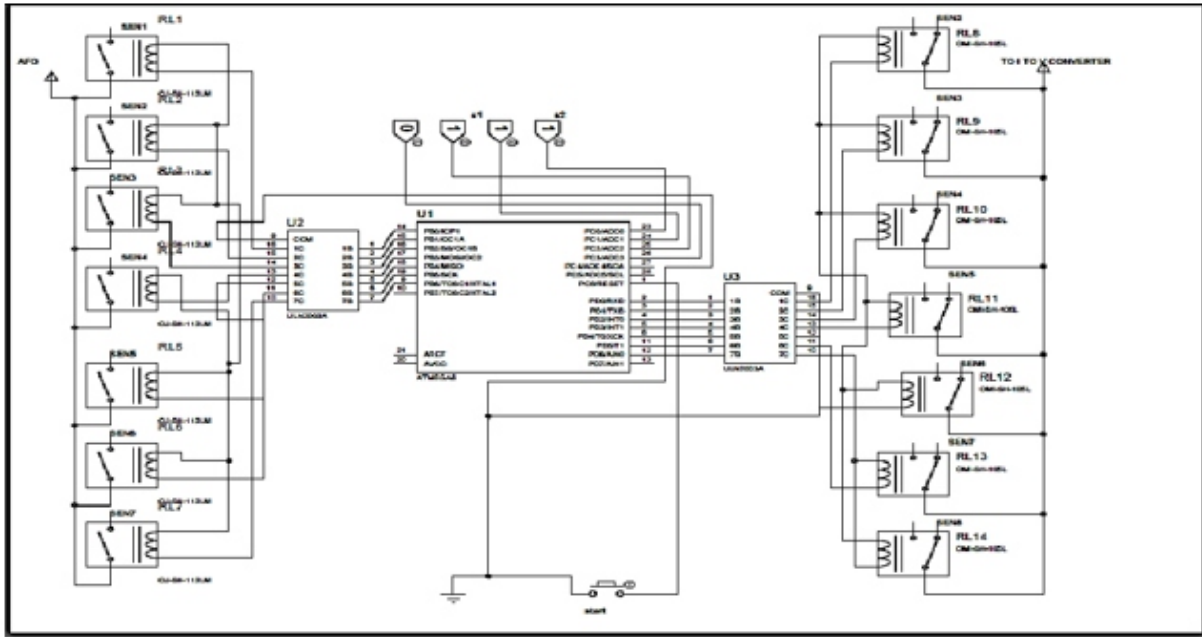


Figure 2. Circuit Diagram for Driving Circuit

4. EXPERIMENTAL RESULTS

The pulse generating circuit is designed for 1 micro second pulse width and 400 nanosecond rise and fall time. The outputs are obtained through embedded system with necessary supporting circuits. The output signal of the differentiator output for different capacitance is measured. The output shows that differentiating output having the noise with the amplitude of 0.2v. The practical output results for programmable gain amplifier are taken for the 3.9 Pf, and the corresponding output voltage is 1V. The results and the response for programmable gain amplifier are shown in the figure 3 and in the experimental setup figure 4.

The circuit for the driving circuit is constructed as per the design. The performance is demonstrated with ECT sensor with full air medium and for different switching signals. Thus the sequence observed at low frequency switching pulses validates the logic used for driving the electrode status. The gain selection for the programmable gain amplifier is checked.

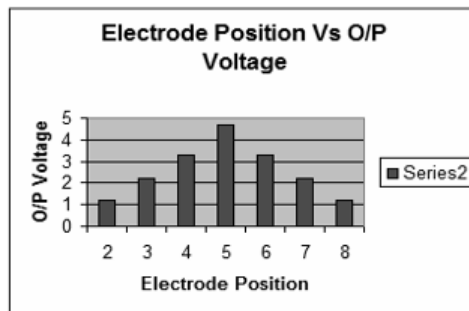


Figure 3. Programmable Gain amplifier response



Figure 4. Experimental work

CONCLUSIONS

In this paper we present high-speed data processing system for AC ECT sensor. This concept is analyzed, considering sensing speed, noise level and accuracy. A signal conditioning circuits can be able to measure a small inter-electrode capacitance in the presence of large stray capacitances giving good stray immunity. The output voltage of the differentiator mainly depends on the unknown capacitance, feedback resistor and excitation voltage. The analog multiplexers can be switched by using interface with programming. The multiplexers are operated with very high speed according to the channel selection by the controller. The embedded system can be operated in the nanoseconds range.

REFERENCES

- [1] Gao Yan-li, Zhang Yongga, *Designing High-speed Hardware for Electrical Capacitance Tomography System, International Form on Computer Science Technology and Application*, 2009, pp.(332-335)
- [2] Kjell Joar Alme and Saba Mylvaganam, *Electrical Capacitance Tomography— Sensor Models, Design, Simulations, and Experimental Verification, IEEE Sensor Journal*, Vol 6, October 2006, PP.(1256-1265)
- [3] Warsito Warsito, Qussai Marashdeh, Liang-Shih Fan, *Electrical Capacitance Volume Tomography, IEEE sensors journal*, Vol. 7, No. 4, April 2007.
- [4] Qi Wang, Huaxiang Wang, Kuihong Hao, and Peng Dai, *Two-Phase Flow Regime Identification Based on Cross-Entropy and Information Extension Methods for Computerized Tomography, IEEE transactions on Instrumentation and measurements*, Vol. 60, No.2, February 2011.
- [5] S.M.Huang, C.G.Xie, R.Thorn.D.Snowden.M.S.Beck, *Design of sensor Electronics for Electrical Capacitance Tomography, IEE Proceedings-G*, Vol.139,1992, PP (83-88)
- [6] S.Sathyamoorthy and J.Sarachandrababu, *Design of High-Speed Pulse Input Based Capacitance Measurement for Electrical Capacitance Tomography, Sensors & Transducers Journal*, Vol.75, Issue 1, January 2007.
- [7] Zhaoyan Fan, Robert X. Gao, *A New Sensing Method for Electrical Capacitance Tomography, IEEE*, 2010
- [8] Ji ying, *Design and implementation of hardware system for electrical Capacitance Tomography, First international workshop on education technology and computer science*, 2009, pp.(588-594)
- [9] Li Lanying, Gao Ming and Chen Deyun, *A Novel Multiple Electrodes Excitation Method For Electrical Capacitance tomography System*. 2011, PP.(1167-1171)
- [10] Zhaoyan Fan, Robert X-Gao *A Frequency selection scheme for increased Imaging speed in ECT, IEEE 2012*
- [11] L. F. M. Moura, E. Cenedese and A. C. Azevedo Filho, *Numerical study of a capacitive tomography system for multiphase flow Thermal engineering vol.8.no.02.December 2007*
- [12] Lijun xu, Halil zhou, Zhang cao and wuqiang yang, *A Digital switching demodulator for electrical capacitance tomography, IEEE transactions on Instrumentation and measurements*, Vol. 62, No.5, May 2013.
- [13] Samir Teniou, Mahmoud Meribout, and Khaled Belarbi *Real-Time Reconstruction of Moving Objects in an Electrical Capacitance Tomography System Using Inter-Frame Correlation, IEEE Sensors Journal*, Vol.12, No.7, July 2012.
- [14] Xia Li, Zhiyao Huang, Baoliang Wang, and Haiqing Li, *A New Method for the Online Voidage Measurement of the Gas–Oil Two-Phase Flow IEEE transaction on instrumentation and measurement*, Vol.58, No. 5, May 2009
- [15] W. Q. Yang, A. L. Stott, and J. C. Gamio, *Analysis of the Effect of Stray Capacitance on an AC-Based Capacitance Tomography Transducer, IEEE transaction on instrumentation and measurement*, Vol.52, No. 5, October 2003

Instructions for Authors

Essentials for Publishing in this Journal

- 1 Submitted articles should not have been previously published or be currently under consideration for publication elsewhere.
- 2 Conference papers may only be submitted if the paper has been completely re-written (taken to mean more than 50%) and the author has cleared any necessary permission with the copyright owner if it has been previously copyrighted.
- 3 All our articles are refereed through a double-blind process.
- 4 All authors must declare they have read and agreed to the content of the submitted article and must sign a declaration correspond to the originality of the article.

Submission Process

All articles for this journal must be submitted using our online submissions system. <http://enrichedpub.com/> . Please use the Submit Your Article link in the Author Service area.

Manuscript Guidelines

The instructions to authors about the article preparation for publication in the Manuscripts are submitted online, through the e-Ur (Electronic editing) system, developed by **Enriched Publications Pvt. Ltd.** The article should contain the abstract with keywords, introduction, body, conclusion, references and the summary in English language (without heading and subheading enumeration). The article length should not exceed 16 pages of A4 paper format.

Title

The title should be informative. It is in both Journal's and author's best interest to use terms suitable. For indexing and word search. If there are no such terms in the title, the author is strongly advised to add a subtitle. The title should be given in English as well. The titles precede the abstract and the summary in an appropriate language.

Letterhead Title

The letterhead title is given at a top of each page for easier identification of article copies in an Electronic form in particular. It contains the author's surname and first name initial .article title, journal title and collation (year, volume, and issue, first and last page). The journal and article titles can be given in a shortened form.

Author's Name

Full name(s) of author(s) should be used. It is advisable to give the middle initial. Names are given in their original form.

Contact Details

The postal address or the e-mail address of the author (usually of the first one if there are more Authors) is given in the footnote at the bottom of the first page.

Type of Articles

Classification of articles is a duty of the editorial staff and is of special importance. Referees and the members of the editorial staff, or section editors, can propose a category, but the editor-in-chief has the sole responsibility for their classification. Journal articles are classified as follows:

Scientific articles:

1. Original scientific paper (giving the previously unpublished results of the author's own research based on management methods).
2. Survey paper (giving an original, detailed and critical view of a research problem or an area to which the author has made a contribution visible through his self-citation);
3. Short or preliminary communication (original management paper of full format but of a smaller extent or of a preliminary character);
4. Scientific critique or forum (discussion on a particular scientific topic, based exclusively on management argumentation) and commentaries. Exceptionally, in particular areas, a scientific paper in the Journal can be in a form of a monograph or a critical edition of scientific data (historical, archival, lexicographic, bibliographic, data survey, etc.) which were unknown or hardly accessible for scientific research.

Professional articles:

1. Professional paper (contribution offering experience useful for improvement of professional practice but not necessarily based on scientific methods);
2. Informative contribution (editorial, commentary, etc.);
3. Review (of a book, software, case study, scientific event, etc.)

Language

The article should be in English. The grammar and style of the article should be of good quality. The systematized text should be without abbreviations (except standard ones). All measurements must be in SI units. The sequence of formulae is denoted in Arabic numerals in parentheses on the right-hand side.

Abstract and Summary

An abstract is a concise informative presentation of the article content for fast and accurate Evaluation of its relevance. It is both in the Editorial Office's and the author's best interest for an abstract to contain terms often used for indexing and article search. The abstract describes the purpose of the study and the methods, outlines the findings and state the conclusions. A 100- to 250-Word abstract should be placed between the title and the keywords with the body text to follow. Besides an abstract are advised to have a summary in English, at the end of the article, after the Reference list. The summary should be structured and long up to 1/10 of the article length (it is more extensive than the abstract).

Keywords

Keywords are terms or phrases showing adequately the article content for indexing and search purposes. They should be allocated heaving in mind widely accepted international sources (index, dictionary or thesaurus), such as the Web of Science keyword list for science in general. The higher their usage frequency is the better. Up to 10 keywords immediately follow the abstract and the summary, in respective languages.

Acknowledgements

The name and the number of the project or programmed within which the article was realized is given in a separate note at the bottom of the first page together with the name of the institution which financially supported the project or programmed.

Tables and Illustrations

All the captions should be in the original language as well as in English, together with the texts in illustrations if possible. Tables are typed in the same style as the text and are denoted by numerals at the top. Photographs and drawings, placed appropriately in the text, should be clear, precise and suitable for reproduction. Drawings should be created in Word or Corel.

Citation in the Text

Citation in the text must be uniform. When citing references in the text, use the reference number set in square brackets from the Reference list at the end of the article.

Footnotes

Footnotes are given at the bottom of the page with the text they refer to. They can contain less relevant details, additional explanations or used sources (e.g. scientific material, manuals). They cannot replace the cited literature.

The article should be accompanied with a cover letter with the information about the author(s): surname, middle initial, first name, and citizen personal number, rank, title, e-mail address, and affiliation address, home address including municipality, phone number in the office and at home (or a mobile phone number). The cover letter should state the type of the article and tell which illustrations are original and which are not.